2010 International Symposium on Nonlinear Theory and its Applications
NOLTA2010, Krakow, Poland, September 5-8, 2010

Numerical Calculation Method of Characteristic Multiplier for the Fixed Point in a Rigid Overhead Wire-Pantograph System

Shota Hirashima†, Shu Karube‡ and Takuji Kousaka†

†Department of Mechanical and Energy Systems Engineering,
Oita University, 700 Dannoharu, Oita, Oita, 870–1192 Japan
‡Oita National College of Technology,
1666 Maki, Oita, 870–0152 Japan
Email: shota@bifurcation.jp, karube@oita-ct.ac.jp, takuji@oita-u.ac.jp

Abstract—We propose a numerical calculation method of characteristic multiplier for the fixed point in a rigid overhead wire-pantograph system. First, we show a rigid overhead wire-pantograph system and explain its dynamics. Then, the Poincaré map is defined by using the local section and some objects. In addition, the fixed point is completely calculated based on the derivative of Poincaré map. Finally, above method is applied for a rigid overhead wire-pantograph system.

1. Introduction

The class of system that switched depending on its own state, including jump phenomena when the orbit hits the border is generally called as the impact oscillator. It is well known that there are variety of nonlinear phenomena in the impact oscillator because of its switching complicity. Also, impact oscillator is classified into two types based on the property of borders. The first type of impact oscillator has the fixed border. Many researchers have investigated the nonlinear dynamics in such class of impact oscillator; mechanical system [1, 2], spiking neuron model in biological system [3, 4], impact model of forest fire in ecosystem [5].

The rigid overhead wire-pantograph system with moving border is classified into the other type of impact oscillator. One of a big problem in the rigid overhead wire-pantograph system is the rail corrugation because it generate a noise and contact loss in the running railway. Thus the qualitative analysis of the rigid overhead wire-pantograph system is an important topic in the engineering field in terms of the practical application. In a previous work, the simplified model of the rigid overhead wire-pantograph system has proposed in Ref. [6]. We also have studied above simplified model, and clarified some basic characteristics in terms of the bifurcation theory [7]. On the other hand, the detailed bifurcation analysis is very difficult because the model is divided in high-dimensional system with nonlinear property. For this reason, there is no result of the detailed bifurcation analysis in the rigid overhead wire-pantograph system.

This paper addresses the first step to completely analyze the bifurcation phenomena in a two-dimensional model [7] from the mathematical point of view. More preciously, the numerical calculation method is constructed based on Ref. [8]. Note that Ref. [8] clarified the analyzing method of bifurcation phenomena for the fixed point in two-dimensional impact oscillator with the fixed border. First, we show the model and explain its dynamics. Then, the Poincaré map is defined by using the local section and some objects. In addition, the fixed point is completely calculated based on the derivative of Poincaré map. Finally, above method is applied for a rigid overhead wire-pantograph system.

2. A Rigid Overhead Wire-Pantograph System

The overhead wire model includes the rail corrugation, and the pantograph model is composed of a spring, damper and mass, respectively. Note that the mass in the pantograph model impacts to the stopper that vibrates periodically. Now, we call stopper as the border in the following analysis. In addition, we assume the initial displacement d in the pantograph model because actual pantograph has the upward force. Let us suppose that the initial displacement d is defined by the equation of static equilibrium in our model. Consequently, the model's equation of motion is shown as follows [6]:

$$\begin{cases} \dfrac{dx}{dt} &= v \\ \dfrac{dv}{dt} &= -x - 2\zeta v + P_n, \end{cases} \tag{1}$$

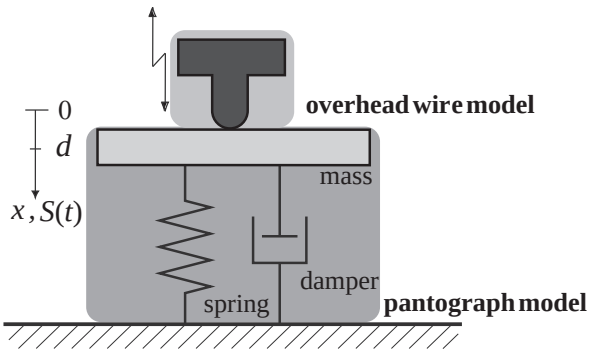

Figure 1: Nonlinear vibration system.

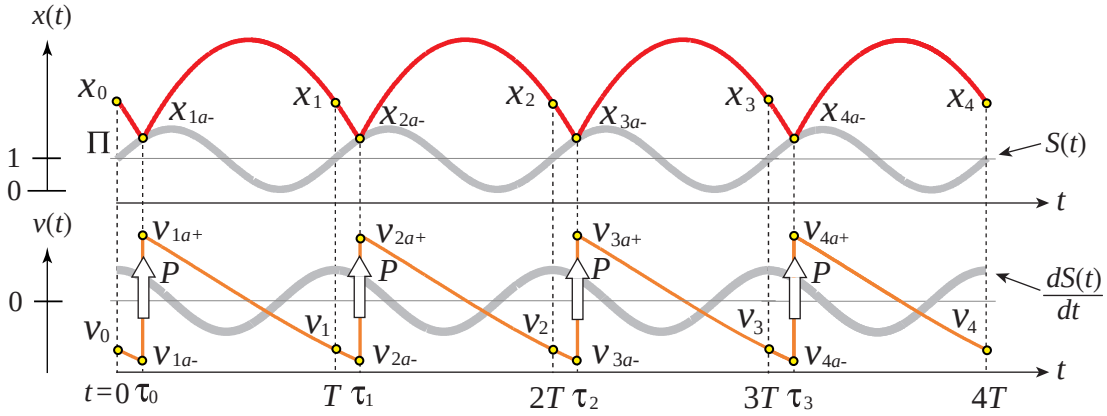

Figure 2: Example of the orbit

where ζ, x and v denote the damping ration, the displacement and the velocity in the pantograph model, respectively. On the other hand, the normalized equation of the overhead wire model is given by

$$S(t) = \varepsilon \sin \Omega t + 1, \tag{2}$$

where the displacement $S(t)$ depends on the amplitude ε and the frequency ratio Ω in the overhead wire model.

Figure 2 shows an example of the orbit. In the upper section of Fig. 2 denotes the displacements of the mass (x) and border ($S(t)$), respectively. Likewise, the lower section of Fig. 2 corresponds to the velocities of the mass (v) and the border ($dS(t)/dt$). The orbit is described by Eq. (1) until the parameter x reaches to $S(t)$. After that the tangential force P_n appears between the pantograph and the overhead wire. Now, P_n is expressed as follows:

$$P_n = \begin{cases} \varepsilon[(1-\Omega^2)\sin\Omega t + 2\zeta\Omega\cos\Omega t] + 1, & x \le S(t), \\ 0, & x > S(t). \end{cases} \tag{3}$$

The orbit during the periodic interval is classified into two types by the state of P_n at time $x = S(t)$. If $P_n > 0$ is satisfied, the pantograph model keeps the state of contact with the overhead wire model. On the other hand, the impact between the pantograph model and overhead wire model can be observed under the condition of $P_n = 0$; and the velocity immediately switches to the positive vector field. Note that v_+ in Eq. 4 denotes the velocity of after the impact.

$$v_+ = -\alpha v_- + (1+\alpha)\frac{dS(t)}{dt} \tag{4}$$

Now, v_- and $dS(t)/dt$ are velocities of x and $S(t)$. Also, α is a coefficient of restitution between the pantograph model and the overhead wire model.

3. Numerical Calculation Method of Characteristic Multiplier

3.1. Poincaré map

We calculate the characteristic multiplier in the rigid overhead wire-pantograph system. First of all, we let the behavior of orbit in the system as follows:

$$\begin{cases} \dfrac{dx}{dt} = f(x, v, \lambda) \\ \dfrac{dv}{dt} = g(x, v, \lambda) \end{cases}, \tag{5}$$

where the parameters t, x, v and λ satisfies $t \in \boldsymbol{R}$, $x, v \in \boldsymbol{R}^2$ $f, g : \boldsymbol{R}^2$ and λ. Now, Eq. (5) is rewritten as follows:

$$\begin{cases} x(t) = \varphi(t; x, v, \lambda), x(0) = x_0 \\ v(t) = \phi(t; x, v, \lambda), v(0) = v_0 \end{cases}, \tag{6}$$

where x_0 and y_0 means the initial value at time $t = 0$. Next, we define the following local section $\Pi \in \boldsymbol{R}^2$ by using scalar functions $q : \boldsymbol{R}^2 \to \boldsymbol{R}^2$.

$$\begin{aligned} &\Pi = \{x, v \in \boldsymbol{R}^2 : q(t, x, v) = 0, q : \boldsymbol{R}^2 \to \boldsymbol{R}^2\}, \\ &q(t+T, x, v) = q(t, x, v) \end{aligned} \tag{7}$$

Also, we assume that the map P gives the following jumping phenomena in the orbit if x reaches to Π.

$$\begin{aligned} &P : \boldsymbol{R}^2 \to \boldsymbol{R}^2, \\ &\begin{bmatrix} x_{1a-} \\ v_{1a-} \end{bmatrix} = \begin{bmatrix} \varphi(\tau_0; x_0, v_0, \lambda) \\ \phi(\tau_0; x_0, v_0, \lambda) \end{bmatrix} \\ &\qquad \mapsto \begin{bmatrix} x_{1a+} \\ v_{1a+} \end{bmatrix} = \begin{bmatrix} r(\tau_0; x_0, v_0) \\ s(\tau_0; x_0, v_0) \end{bmatrix} \end{aligned} \tag{8}$$

τ_0 is the time when the orbit reaches to Π. The orbit $\boldsymbol{x}_1$ at the time T is expressed as follow:

$$\boldsymbol{x}_1 = \begin{bmatrix} x_1 \\ v_1 \end{bmatrix} = \begin{bmatrix} \varphi(T - \tau_0; x_{1a+}, v_{1a+}, \lambda) \\ \phi(T - \tau_0; x_{1a+}, v_{1a+}, \lambda) \end{bmatrix}. \tag{9}$$

Next, we define the map.

$$\begin{aligned} M_0 &: \boldsymbol{R}^2 \to \Pi, \ (x_0, v_0) \mapsto (x_{1a-}, v_{1a-}) \\ M_1 &: \Pi \to \boldsymbol{R}^2, \ (x_{1a+}, v_{1a+}) \mapsto (x_1, v_1). \end{aligned} \tag{10}$$

Consequently, the Poincaré map is given by

$$\begin{aligned} M : \ &\boldsymbol{R}^2 \to \boldsymbol{R}^2 \\ &(x_0, v_0) \mapsto (x_1, v_1) = M_1 \circ P \circ M_0. \end{aligned} \tag{11}$$

In the following analysis, we discuss the derivative of the Poincaré map. Eq. (11), is rewritten as follows:

$$\begin{aligned} DM(x_0, v_0) &= \begin{bmatrix} \dfrac{\partial M(x_0)}{\partial x_0} & \dfrac{\partial M(x_0)}{\partial v_0} \\ \dfrac{\partial M(v_0)}{\partial x_0} & \dfrac{\partial M(v_0)}{\partial v_0} \end{bmatrix} \\ &= \begin{bmatrix} \left.\dfrac{\partial \varphi}{\partial t}\right|_{t=T-\tau_0} \\ \left.\dfrac{\partial \phi}{\partial t}\right|_{t=T-\tau_0} \end{bmatrix} \begin{bmatrix} -\dfrac{\partial \tau_0}{\partial x_0} & -\dfrac{\partial \tau_0}{\partial v_0} \end{bmatrix} \\ &\quad + \begin{bmatrix} \dfrac{\partial \varphi}{\partial x_{1a+}} & \dfrac{\partial \varphi}{\partial v_{1a+}} \\ \dfrac{\partial \phi}{\partial x_{1a+}} & \dfrac{\partial \phi}{\partial v_{1a+}} \end{bmatrix} \begin{bmatrix} \dfrac{\partial r}{\partial x_0} & \dfrac{\partial r}{\partial v_0} \\ \dfrac{\partial s}{\partial x_0} & \dfrac{\partial s}{\partial v_0} \end{bmatrix}. \end{aligned} \tag{12}$$

Now, derivative of the function P is given by follows depending on the initial value.

$$\begin{aligned} \begin{bmatrix} \dfrac{\partial r}{\partial x_0} & \dfrac{\partial r}{\partial v_0} \\ \dfrac{\partial s}{\partial x_0} & \dfrac{\partial s}{\partial v_0} \end{bmatrix} &= \begin{bmatrix} \left.\dfrac{\partial r}{\partial t}\right|_{t=\tau_0} \\ \left.\dfrac{\partial s}{\partial t}\right|_{t=\tau_0} \end{bmatrix} \begin{bmatrix} \dfrac{\partial \tau_0}{\partial x_0} & \dfrac{\partial \tau_0}{\partial v_0} \end{bmatrix} \\ &\quad + \begin{bmatrix} \dfrac{\partial x_{1a+}}{\partial x_{1a-}} & \dfrac{\partial x_{1a+}}{\partial v_{1a-}} \\ \dfrac{\partial v_{1a+}}{\partial x_{1a-}} & \dfrac{\partial v_{1a+}}{\partial v_{1a-}} \end{bmatrix} \begin{bmatrix} \dfrac{\partial x_{1a-}}{\partial x_0} & \dfrac{\partial x_{1a-}}{\partial v_0} \\ \dfrac{\partial v_{1a-}}{\partial x_0} & \dfrac{\partial v_{1a-}}{\partial v_0} \end{bmatrix} \end{aligned} \tag{13}$$

Moreover,

$$\begin{aligned} \begin{bmatrix} \dfrac{\partial x_{1a-}}{\partial x_0} & \dfrac{\partial x_{1a-}}{\partial v_0} \\ \dfrac{\partial v_{1a-}}{\partial x_0} & \dfrac{\partial v_{1a-}}{\partial v_0} \end{bmatrix} &= \begin{bmatrix} \left.\dfrac{\partial \varphi}{\partial t}\right|_{t=T-\tau_0} \\ \left.\dfrac{\partial \phi}{\partial t}\right|_{t=T-\tau_0} \end{bmatrix} \begin{bmatrix} \dfrac{\partial \tau_0}{\partial x_0} & \dfrac{\partial \tau_0}{\partial v_0} \end{bmatrix} \\ &\quad + \begin{bmatrix} \dfrac{\partial \varphi}{\partial x_0} & \dfrac{\partial \varphi}{\partial v_0} \\ \dfrac{\partial \phi}{\partial x_0} & \dfrac{\partial \phi}{\partial v_0} \end{bmatrix}. \end{aligned} \tag{14}$$

We should remark that the function

$$q(\tau_0; x_0, v_0) = x_{1a-} - S(t) = 0, \tag{15}$$

is differentiable for $\boldsymbol{x}_0$. Hence, $\dfrac{\partial q}{\partial \boldsymbol{x}_0}$ can be obtained as

$$\begin{aligned} \frac{\partial q}{\partial \boldsymbol{x}_0} &= \begin{bmatrix} \dfrac{\partial q}{\partial x_0} & \dfrac{\partial q}{\partial v_0} \end{bmatrix} \\ &= \begin{bmatrix} \left.\dfrac{\partial q}{\partial t}\right|_{t=\tau_0} \dfrac{\partial \tau_0}{\partial x_0} & \left.\dfrac{\partial q}{\partial t}\right|_{t=\tau_0} \dfrac{\partial \tau_0}{\partial v_0} \end{bmatrix} \\ &\quad + \begin{bmatrix} \dfrac{\partial q}{\partial x} & \dfrac{\partial q}{\partial v} \end{bmatrix} \begin{bmatrix} \dfrac{\partial x_{1a-}}{\partial x_0} & \dfrac{\partial x_{1a-}}{\partial v_0} \\ \dfrac{\partial y_{1a-}}{\partial x_0} & \dfrac{\partial y_{1a-}}{\partial v_0} \end{bmatrix} = \boldsymbol{0}, \end{aligned} \tag{16}$$

$\dfrac{\partial \tau_0}{\partial x_0}$ and $\dfrac{\partial \tau_0}{\partial v_0}$ become

$$\begin{bmatrix} \dfrac{\partial \tau_0}{\partial x_0} \\ \dfrac{\partial \tau_0}{\partial v_0} \end{bmatrix} = \begin{bmatrix} \dfrac{-\left(\dfrac{\partial q}{\partial x}\dfrac{\partial \varphi}{\partial x_0} + \dfrac{\partial q}{\partial v}\dfrac{\partial \phi}{\partial x_0}\right)}{\dfrac{\partial q}{\partial x}\left.\dfrac{\partial \varphi}{\partial t}\right|_{t=\tau_0} + \dfrac{\partial q}{\partial y}\left.\dfrac{\partial \phi}{\partial t}\right|_{t=\tau_0} + \left.\dfrac{\partial q}{\partial t}\right|_{t=\tau_0}} \\ \dfrac{-\left(\dfrac{\partial q}{\partial x}\dfrac{\partial \varphi}{\partial v_0} + \dfrac{\partial q}{\partial v}\dfrac{\partial \phi}{\partial v_0}\right)}{\dfrac{\partial q}{\partial x}\left.\dfrac{\partial \varphi}{\partial t}\right|_{t=\tau_0} + \dfrac{\partial q}{\partial y}\left.\dfrac{\partial \phi}{\partial t}\right|_{t=\tau_0} + \left.\dfrac{\partial q}{\partial t}\right|_{t=\tau_0}} \end{bmatrix}. \tag{17}$$

A fixed point of the Poincaré map is given by

$$\boldsymbol{x}_0 - M(\boldsymbol{x}_0) = 0. \tag{18}$$

The characteristic equation for the fixed point is expressed

$$\chi(\mu) = |\mu \boldsymbol{I}_n - DM(\boldsymbol{x}_0)| = 0. \tag{19}$$

We can obtain the location and stability of fixed point when Eqs. (18) and (19) are solved by arbitrarily numerical calculation method.

3.2. Application result

Figure 3 shows the example of the orbit and phase plane with various Ω. In this figure, we can observe that the fixed point bifurcate to the period-2 orbit via the period doubling bifurcation. Now, we pay attention to above period doubling bifurcation, and apply our method for the fixed point. More preciously, we calculate Eqs. (18) and (19). Table 1 shows the analytical result; the fixed point and characteristic multiplier μ_1 and μ_2. Consequently, we conclude that the period doubling bifurcation is occur at $\Omega = 4.57641$, After that the fixed point becomes unstable, and the period-2 orbit is generated. Here, Fig. 4 shows the one-dimensional bifurcation diagram at $\zeta = 0.049$. Likewise, the period doubling bifurcation is observed at $\Omega = 4.57641$ in this figure. To that end, we can realize that our method proposed in the previous section may applicable to the analysis of stability for the period-n ($n \geq 2$) orbit in the rigid overhead wire-pantograph system.

4. Conclusion

In this paper, we have proposed the numerical calculation method of characteristic multiplier for the fixed point in the rigid overhead wire-pantograph system. First, we explained the model and derived the the Poincaré map. Then, the fixed point was completely calculated based on the derivative of Poincaré map. Finally, we applied our method to the rigid overhead wire-pantograph system. As a result, our method's validity was confirmed. Also, we consider that our method proposed in this paper may applicable to the analysis of stability for the period-n ($n \geq 2$) orbit in the rigid overhead wire-pantograph system. Our future work to be studied is to calculate the stability of the period-n ($n \geq 2$) orbit.

Table 1: Calculation of the fixed point and characteristic multiplier with Ω ($\zeta = 0.049$).

Ω	μ_1	μ_2	Remarks
4.45798	-0.02840	-0.73682	Stable
4.48592	-0.02619	-0.79956	Stable
4.51550	-0.02422	-0.86545	Stable
4.56359	-0.02160	-0.97177	Stable
4.56804	-0.02139	-0.98157	Stable
4.57201	-0.02120	-0.99031	Stable
⋮	⋮	⋮	⋮
4.57641	-0.02100	-1.00000	Period-doubling bifurcation
⋮	⋮	⋮	⋮
4.58033	-0.02082	-1.00861	Unstable

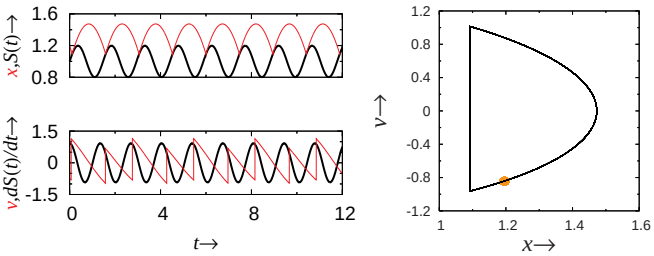

(a) Fixed point ($\Omega = 4.27$)

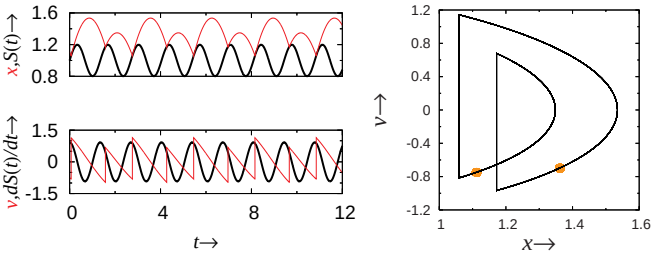

(b) Period-2 orbit ($\Omega = 4.66$)

Figure 3: Orbits and phase plane ($\zeta = 0.049$).

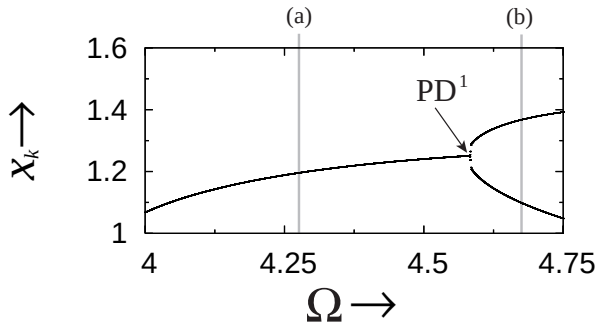

Figure 4: One-dimensional bifurcation diagram ($\zeta = 0.049$).

Acknowledgment

The authors would like to thank Prof. Y. Yoshitake of Nagasaki University, Prof. T. Ueta of The University of Tokushima and Assist. Prof. K. Tsumoto of Osaka University for their valuable discussion. This work is partially supported by the Grant-in-Aid for Young Scientists B (KAKENHI) and Research Fund at the Discretion of the President, Oita University.

References

[1] Barbara Blazejczyk-Okolewska, "Analysis of an impact damper of vibrations," *Chaos, Solitons and Fractals*, vol. 12, no. 11, pp. 1983–1988, 2000.

[2] J. Park, S. Wang, and M. J. Crocker, "Mass loaded resonance of a single unit impact damper caused by impacts and the resulting kinetic energy influx," *Journal of Sound and Vibration*, vol. 323, no. 3-5, pp. 877–895, 2009.

[3] Y. D. Sato and M. Shiino, "Generalization of coupled spiking models and effects of the width of an action potential on synchronization phenomena," *Phys. Rev. E*, vol. 75, 011909, 2007.

[4] E. M. Izhikevich, "Simple model of spiking neurons," *IEEE Trans. Neural Netw.* , vol. 14, no. 6, pp. 1569–1572, 2003.

[5] S. Maggi and S. Rinaldi, "A second-order impact model for forest fire regimes," *Theoretical Population Biology*, vol. 70, no. 2, pp. 174–182, 2006.

[6] S. Kawamura, K. Kitajo, S. Horita and M. Yoshizawa, "Fundamental Study on Impact Oscillations of Rigid Trolley-Pantograph System," *The Japan Society of Mechanical Engineers, Series C*, vol. 73, no. 728, pp. 974–981, 2007(In Japanese).

[7] I. Nishinaga, S. Tomonaga, S. Karube and T. Kousaka, "Fundamental Property of a Nonlinear Vibration System
Based on a Rigid Overhead Wire-Pantograph System," International Conference on Communications, Circuits and Systems, pp.868–871, 2009.

[8] S. Tomonaga, K. Tsumoto, T. Kousaka, "Analyzing Method of Bifurcation Phenomena for Two-dimensional Impact Oscillators with Fixed Border," 2009 International Symposium on Nonlinear Theory and its Applications, pp.187–190, 2009.